Expression and effects of inhibition of type I insulin-like growth factor receptor tyrosine kinase in mantle cell lymphoma

Deeksha Vishwamitra,[1,2] Ping Shi,[1,3] Desiree Wilson,[1] Roxsan Manshouri,[1] Francisco Vega,[1] Ellen J. Schlette,[1] and Hesham M. Amin[1,2]

[1]Department of Hematopathology, the University of Texas M. D. Anderson Cancer Center, Houston, Texas, USA; [2]the University of Texas Graduate School of Biomedical Sciences, Houston, Texas, USA, and [3]State Key Laboratory of Bioreactor Engineering, East China University of Science and Technology, Shanghai, China

Acknowledgments: the authors would like to thank Ms. Wei Qiao from the Department of Biostatistics at the University of Texas M. D. Anderson Cancer Center for her excellent assistance with the statistical analysis.

Funding: DW is supported by Minority Access to Research Careers Fellowship (T34GM079088) from the National Institutes of Health (NIH). The work is supported by CA114395 grant from the NIH and by the Physician Scientist Program Award from the University of Texas M.D. Anderson Cancer Center to HMA. The authors declare that they have no financial interests in relation to the work described in this paper.

Manuscript received on August 3, 2010. Revised version arrived on January 24, 2011. Manuscript accepted on February 15, 2011.

Correspondence: Hesham M. Amin, Department of Hematopathology, Unit 72, The University of Texas M.D. Anderson Cancer Center, 1515 Holcombe Boulevard Houston, Texas 77030 USA. E-mail: hamin@mdanderson.org

The online version of this article has a Supplementary Appendix.

ABSTRACT

Background

Type I insulin-like growth factor receptor (IGF-IR) tyrosine kinase induces significant oncogenic effects. Strategies to block IGF-IR signaling are being tested in clinical trials that include patients with aggressive solid malignancies. Mantle cell lymphoma is a B-cell neoplasm with poor prognosis and a tendency to develop resistance. The expression and potential significance of IGF-IR in mantle cell lymphoma are not known.

Design and Methods

We used reverse transcriptase polymerase chain reaction, quantitative real-time polymerase chain reaction, immunoprecipitation, western blotting, flow cytometry, and immunohistochemistry to analyze the expression of *IGF-IR* mRNA, and IGF-IR and pIGF-IR proteins in mantle cell lymphoma cell lines and patients' specimens. Selective and specific blockade of IGF-IR was achieved using picropodophyllin and short-interfering RNA, respectively. Cell viability, apoptosis, cell cycle, cellular morphology, cell proliferation, and target proteins were then analyzed.

Results

We detected the expression of IGF-IR and pIGF-IR in mantle cell lymphoma cell lines. Notably, IGF-IR molecules/cell were markedly increased in mantle cell lymphoma cell lines compared with human B-lymphocytes. IGF-IR and pIGF-IR were also detected in 78% and 74%, respectively, of 23 primary mantle cell lymphoma specimens. Treatment of serum-deprived mantle cell lymphoma cell lines with IGF-I salvaged these cells from apoptosis. Selective inhibition of IGF-IR by picropodophyllin decreased the viability and proliferation of mantle cell lymphoma cell lines, and induced apoptosis and cell cycle arrest. Selective inhibition of IGF-IR was associated with caspase-3, caspase-8, caspase-9, and PARP cleavage, cytochrome c release, up-regulation of cyclin B1, and down-regulation of cyclin D1, pCdc2, pIRS-1, pAkt, and pJnk. Similar results were obtained by using IGF-IR short-interfering RNA. In addition, picropodophyllin decreased the viability and proliferation of primary mantle cell lymphoma cells that expressed IGF-IR.

Conclusions

IGF-IR is up-regulated and frequently activated in mantle cell lymphoma. Our data suggest that IGF-IR could be a molecular target for the treatment of mantle cell lymphoma.

Key words: mantle cell lymphoma, IGF-IR, picropodophyllin, AXL1717, rituximab.

Citation: Vishwamitra D, Shi P, Wilson D, Manshouri R, Vega F, Schlette EJ, and Amin HM. Expression and effects of inhibition of IGF-IR tyrosine kinase in mantle cell lymphoma. Haematologica 2011;96(6):871-880. doi:10.3324/haematol.2010.031567

Introduction

The type I insulin-like growth factor receptor (IGF-IR) tyrosine kinase is composed of two identical α and two identical β subunits connected by disulfide bonds to form the functional transmembranous homodimeric protein complex.[1,2] It is thought that ligand binding causes phosphorylation of tyrosine residues 1131, 1135, and 1136 present in the activation loop of the kinase domain in the β subunit.[3] This biochemical event is subsequently followed by phosphorylation and activation of downstream signaling cascades such as IRS-1/m-TOR/PI3K/Akt, Grb/Ras/MAPK, and JAK/STAT.[4-7]

IGF-IR contributes significantly to the development and progression of malignant tumors and to the emergence of therapeutic resistance.[8] IGF-IR induces its oncogenic effects through inhibition of apoptosis and induction of transformation.[9] Recent studies have claimed that a constitutively active IGF-IR can induce ligand-independent tumor cell progression and may be critically necessary in maintaining the activation of certain oncogenes during the transformation process.[10,11] These effects have been extensively investigated in a variety of solid tumors including breast, prostate, lung, ovary, skin, and soft tissue cancers.[12-16] It is not surprising, therefore, that inhibitors of IGF-IR are currently being evaluated in several clinical trials enrolling patients with some of the most aggressive and resistant types of solid cancers, and some of these inhibitors have shown promising effects.[17,18] It is of note that, in contrast to the widely studied solid tumors, not so many studies have been performed to systematically explore a role of IGF-IR in hematologic neoplasms. To the best of our knowledge, most such studies focused on plasma cell myeloma while many fewer studies examined IGF-IR signaling in lymphoma and leukemia.[19-25]

Mantle cell lymphoma (MCL) is a lymphoid neoplasm of B-cell immunophenotype. It is distinguished by a primary genetic event, namely the chromosomal translocation t(11;14)(q13;q32). This translocation juxtaposes the proto-oncogene *CCND1* at chromosome 11q13 to the *IgH* gene at chromosome 14q32.[26,27] Clinically, MCL constitutes 5 to 10% of all non-Hodgkin's lymphomas, affects more frequently older men, and occurs at an approximate frequency of 3,500 new cases per year in the USA. No curative therapy exists for MCL and there is no consensus on treatment strategies, which are largely nonspecific.[28] These strategies include different chemotherapy combinations plus rituximab (R), such as R-CHOP or the more aggressive regimen R-hyper-CVAD. MCL is one of the most problematic types of malignant lymphoma because it is difficult to treat and patients commonly have a poor outcome after they develop resistance and/or relapse to current therapeutics. In the present study, we evaluated the role of IGF-IR in MCL. We analyzed the expression and activation of IGF-IR in MCL cell lines and patients' tumor samples. We also tested the effects of antagonism of IGF-IR signaling in MCL.

Design and Methods

Cell lines and antibodies

Three previously characterized MCL cell lines were studied: SP-53, Mino, and JeKo-1.[29] Detailed information on other cell lines and the antibodies are included in the *Online Supplementary Methods.*

Treatments

Selective inhibition of IGF-IR was achieved by using the cyclolignan picropodophyllin (PPP; 407247; Calbiochem, Gibbstown, NJ, USA). PPP was prepared and dissolved in ethanol (less than 0.4% by volume) to a final concentration of 0.5 mM. For IGF-IR short interfering (si) RNA knockdown experiments, cells were transiently transfected with SMARTpool designed siRNA (a mixture of 4 different constructs; M-003012-04; Dharmacon, Lafayette, CO, USA). The siCONTROL Non-Targeting siRNA was used as a negative control (D-001206-13-20; Dharmacon). Transfection of the cells by siRNA was performed using the Nucleofector "R" solution for JeKo-1 and "T" solution for Mino and SP-53, as recommended by the manufacturer (A-023 program for JeKo-1, T-001 for Mino, O-017 for SP-53; Amaxa Biosystems, Basel, Switzerland). Because IGF-I is present in fetal bovine serum, 4.0×10^5 cells/mL of MCL cell lines were maintained in serum-free medium for 24 h. Cells were treated with exogenous IGF-I (291-G1-050; R&D Systems, Minneapolis, MN, USA) at a concentration of 500 ng/mL with or without 5 μg/mL of anti-IGF-IR blocking antibody (MAB391; R&D Systems). In some experiments, cells were treated with rituximab (100 μg/mL, NDC 50242-051-21; Cardinal Health, Dublin, OH), and were also incubated during the treatment with 10% human AB serum (100-318; Gemini Bio-Products, Calabasas, CA, USA) as previously described.[30-32]

Polymerase chain reaction analyses, antigen density and western blots

The details of the reverse transcriptase polymerase chain reaction (RT-PCR) and quantitative real time polymerase chain reaction (qPCR) analyses are given in the *Online Supplementary Methods*, together with the method for measuring IGF-IR antigen density on the cells and the details of the western blotting and immunoprecipitation studies.

Tumor samples, tissue microarray, immunohistochemical staining, and cell sorting

Tumor samples available from 23 patients (22 tissues and 4 peripheral blood samples) with a documented diagnosis of MCL were studied after approval of the Institutional Review Board at the M. D. Anderson Cancer Center. Immunohistochemical staining was performed on formalin-fixed paraffin-embedded sections obtained from cell-blocks of cell lines or the human tumors using a DakoCytomation kit (Carpinteria, CA, USA) as previously described.[22,23,33,34] Additional information on immunohistochemical staining is given in the *Online Supplementary Methods*.

In some experiments, cell sorting was performed to separate the MCL cells from peripheral blood samples collected from patients in the leukemic phase of MCL. Cells were simultaneously labeled with the anti-human CD5 and CD19 antibodies (*555355*, *555412*, respectively; BD Biosciences). Cells expressing CD5 and CD19 were sorted using flow cytometry (BD FACSAria IIU Cell Sorter; BD Biosciences).

Other methods and statistical analysis

Exclusion of staining with trypan blue dye, apoptosis and cell cycle analysis, measurement of tyrosine kinase activity, the MTS assay and statistical analysis of the data are described in the *Online Supplementary Methods.*

Results

Expression of IGF-IR and pIGF-IR in mantle cell lymphoma cell lines and patients' samples

RT-PCR studies showed that IGF-IRα (Figure 1A) and IGF-IRβ (Figure 1B) mRNA were over-expressed in MCL cell lines compared to in normal human B-lymphocytes, which demonstrated very low levels of expression. The expression of IGF-IRα was more pronounced in the JeKo-1 and Mino cell lines than in the SP-53 cell line. The positive control cell lines P6 and Karpas 299 expressed IGF-IRα and IGF-IRβ mRNA. Whereas the negative control cell line R^- was completely negative for IGF-IRα mRNA, it did express very low levels of IGF-IRβ mRNA. Similar findings were made in other recent studies and it was suggested that some subclones of R^- cells may maintain the ability to express very low levels of the IGF-IRβ subunit.[22,23,35] Because the R^- cell line lacks the extracellular IGF-IRα subunit, very low levels of expression of IGF-IRβ would most likely not have significant functional effects.

Consistent with the RT-PCR results, immunohistochemical staining demonstrated the expression of IGF-IRβ protein in MCL cell lines (Figure 1C). The cell lines R^- and Karpas 299 were used as negative and positive controls, respectively. Figure 1D shows that the density of IGF-IRα molecules per cell in MCL cell lines was increased to 420 times its level in normal human B-lymphocytes. The expression of IGF-IR protein in MCL cell lines was additionally demonstrated by using anti-IGF-IRβ antibody for immunoprecipitation followed by anti-IGF-IRβ antibody for western blotting (Figure 1E, left panel). Furthermore, we detected the expression of pIGF-IR in the MCL cell lines by using the anti-IGF-IRβ antibody for immunoprecipitation followed by anti-pTyr antibody for western blotting (Figure 1E, left panel). The positive control Karpas 299 cell line expressed IGF-IR and pIGF-IR, whereas the R^- cell line was completely negative for both proteins. Densitometric analysis demonstrated that the pIGF-IR represented 50%, 46%, 57%, and 72% of basal IGF-IR in SP-53, JeKo-1, Mino, and Karpas 299 cell lines, respectively (Figure 1E, right panel). Western blot analysis showed the expression of IGF-IR and pIGF-IR in MCL cell lines cultured in serum-deprived medium for 24 h (Figure 1F). qPCR studies also demonstrated the expression of *IGF-IR* mRNA in these cell lines when cultured in the serum-deprived cell lines (*data not shown*). R^- and Karpas 299 cell lines were used as negative and positive controls, respectively, for the expression of IGF-IR and pIGF-IR.

We also examined the expression of IGF-IR and pIGF-IR proteins in a cohort of primary lymphoma specimens that included 22 tissue and bone marrow specimens and 4 peripheral blood samples collected from 23 MCL patients. Demographic data, specimen types, clinical presentations at time of biopsies, and status of expression of IGF-IR and pIGF-IR are shown in Table 1. Males accounted for 78% (18/23) of the patients. The age of the patients at biopsy ranged between 46 and 88 years, with a median of 65 years. Of the studied specimens, 70% (16/23) were from relapsed/resistant MCL patients, and 30% (7/23) were diagnostic specimens collected from patients at first presentation. IGF-IR was expressed in 78% (18/23) of the specimens. pIGF-IR was expressed in 94% (17/18) of the IGF-IR-positive specimens and in 74% (17/23) of all specimens. Of the IGF-IR- or pIGF-IR-positive specimens, 72% (13/18) were from patients who presented with relapsed/resistant MCL. Figure 1G illustrates two examples of MCL specimens that were simultaneously positive for IGF-IR and pIGF-IR (panels 1 and 2) and an MCL tumor that was positive for IGF-IR and negative for pIGF-IR (panel 3). A reactive lymph node stained for IGF-IR and pIGF-IR is shown (panel 4). Because tumor tissues were not available from patient 23 (Table 1), western blot analysis of peripheral blood MCL cells was performed and demonstrated the expression of IGF-IR and pIGF-IR (Figure 1G).

Lack of expression of IGF-I in mantle cell lymphoma cell lines

RT-PCR was performed to analyze the expression of IGF-I mRNA, the primary ligand of IGF-IR, in MCL cell lines using two different sets of primers to confirm the results. Compared with the positive control K562 cell line, we found no expression of IGF-I in MCL cell lines JeKo-1 and Mino, and very weak expression in SP-53 (Figure 2A). RSC96, Karpas 299, and R^- cell lines were included as negative controls. These results were confirmed by qPCR (Figure 2B).

IGF-I salvages serum-deprived mantle cell lymphoma cell lines from apoptotic cell death

Although IGF-I appears not to be expressed in MCL cell lines, we were still curious to know whether the IGF-IR signaling axis is functional in MCL. Serum-deprived MCL cell lines were treated with IGF-I (500 ng/mL) for 24 h (SP-53) or 36 h (Mino) and apoptosis was analyzed using annexin-V and propidium iodide (PI) labeling. Cells were considered apoptotic if they were annexin-V^+ or annexin-V^+/PI^+. IGF-I decreased apoptosis in serum-deprived MCL cell lines (Figure 2C). These effects were reversed when the cells were simultaneously treated with IGF-I and anti-IGF-IR blocking antibody (5 μg/mL).

Selective inhibition of IGF-IR by picropodophyllin induces cell death in mantle cell lymphoma

To test whether IGF-IR contributes to the survival of MCL, PPP, a selective inhibitor of IGF-IR, was used. At 24 h, PPP down-regulated pIGF-IR in a concentration-dependent manner without altering baseline IGF-IR levels (the Mino cell line is shown as a representative example, Figure 3A). At 24 h, IGF-IR tyrosine kinase activity also decreased in MCL cell lines in a concentration-dependent fashion (Figure 3B). The decrease in pIGF-IR and IGF-IR tyrosine kinase activity was associated with concentration- and time-dependent decreases in cell viability (Figure 4A). At 48 h after treatment, IC_{50} values were 1.2 μM for Mino and 1.7 μM for SP-53 and JeKo-1 (Figure 4A, lower panel). PPP did not decrease the viability of normal human B-lymphocytes.

Treatment with PPP also induced apoptosis in MCL cell lines (Figure 4B). At 24 h, apoptosis of SP-53, JeKo-1, and Mino cell lines was increased by 1.7-, 3.5-, and 3.0-fold, respectively, relative to untreated cells (Figure 4B, upper panel). At 48 h, apoptosis of SP-53, JeKo-1, and Mino cells lines was increased by 3.0-, 5.5-, and 6.3-fold, respectively, compared to control untreated cells (Figure 4B, lower panel). Cell cycle analysis revealed that PPP induced a G2/M-phase cell cycle arrest in MCL cell lines after 24 h of treatment (Figure 4C). Morphological changes associated with apoptosis and G2/M-phase cell cycle arrest were detected by staining cytospin slides with Giemsa (Figure 4D).

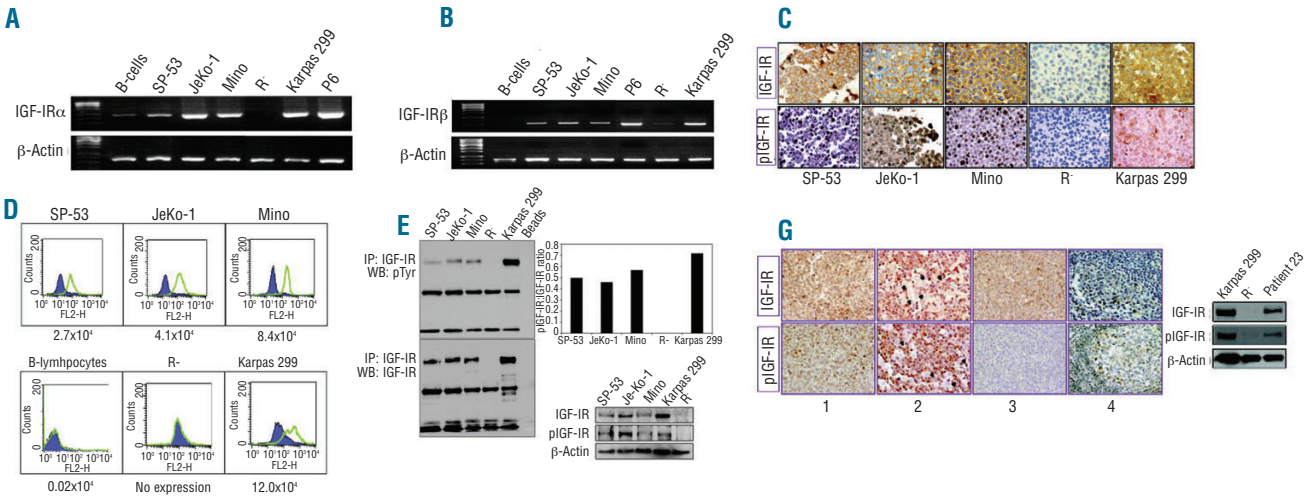

Figure 1. Expression of IGF-IR and pIGF-IR in MCL cell lines and human samples. RT-PCR showed the expression of IGF-IRα (A) and IGF-IRβ mRNA (B) in three MCL cell lines. The cell lines Karpas 299 and P6 were used as positive controls. In contrast, very low levels of IGF-IRα and IGF-IRβ mRNA were detected in B-lymphocytes and very low levels of IGF-IRβ were detected in the R⁻ cell line. The expression of IGF-IRβ and pIGF-IR proteins was documented in the MCL cell lines by using immunohistochemical staining (original magnification: ×400) (C). The cell lines R⁻ and Karpas 299 were used as negative and positive controls, respectively. Flow cytometry measuring relative IGF-IR antigen density per cell demonstrated an up to 420-fold increase in the expression of IGF-IRα molecules per cell in MCL cell lines compared with in normal human B-lymphocytes. R⁻ and Karpas 299 cell lines were used as negative and positive controls, respectively (D). Expression of IGF-IRα is represented by the green peaks and the IgG_1 isotypic control by the purple areas. Estimated numbers of IGF-IR molecules per cell are shown. Immunoprecipitation followed by western blotting demonstrated the expression of pIGF-IR and IGF-IR in SP-53, JeKo-1, and Mino cell lines. The R⁻ and Karpas 299 cell lines were used as negative and positive controls, respectively (E, left panel). Densitometric analysis shows that pIGF-IR represented 50%, 46%, 57%, and 72% of total IGF-IR in SP-53, JeKo-1, Mino, and Karpas 299 cell lines, respectively (E, right panel). Western blot studies show the expression of IGF-IR and pIGF-IR in MCL cell lines after culture in serum-deprived medium for 24 h. R⁻ and Karpas 299 cell lines were used as negative and positive controls, respectively (F). Immunohistochemical staining demonstrated the expression of IGF-IR and pIGF-IR in 78% and 74%, respectively, of MCL primary specimens. Panels 1 and 2 illustrate two cases that were positive for IGF-IR and pIGF-IR, and panel 3 depicts a case that was positive for IGF-IR and negative for pIGF-IR (original magnification: ×400). The black arrowheads in panel 2 highlight interstitial histiocytes that were negative for both IGF-IR and pIGF-IR proteins. Panel 4 shows the expression of IGF-IR and pIGF-IR in a reactive lymph node. IGF-IR and pIGF-IR were weakly expressed in some of the large lymphocytes within the germinal center, and strongly expressed in scattered plasma cells and lymphoplasmacytoid lymphocytes. Because of lack of tumor tissue material from patient 23, western blotting was performed on MCL cells from a peripheral blood sample, and showed the expression of IGF-IR and pIGF-IR (G).

Furthermore, treatment of MCL cell lines by PPP induced a concentration-dependent decrease in cell proliferation at 24 h, which was more pronounced at 48 h after treatment. The effect of PPP was more evident in JeKo-1 and Mino cell lines than in the SP-53 cell line (Figure 4E).

We also sought to compare the effects of treatment with PPP or rituximab alone *versus* the effects of combined treatment with both agents. At 48 h, rituximab and PPP decreased the viability of JeKo-1 cells to 78% and 37%, respectively, of the baseline level. Importantly, simultaneous treatment with PPP and rituximab resulted in only 16% cell viability (Figure 4F, upper panel). The differences among the treatments were also detected when apoptosis was analyzed. After 24 h, rituximab and PPP induced 1.2- and 2.8-fold increases, respectively, in apoptotic cells compared to an increase of 3.9-fold when both agents were used simultaneously (Figure 4F, lower panel).

Thus far, the experiments in cell lines suggested that targeting IGF-IR could be a possible approach to treat MCL patients. To examine this possibility further, we performed experiments in primary MCL tumor cells selected by cell sorting from four peripheral blood samples. At 24 h, PPP induced concentration-dependent decreases in the viability and proliferation of IGF-IR-expressing cells (from patients 21, 22, and 23 in Table 1) (Figure 4G). Importantly, PPP failed to induce these effects in primary MCL cells that were negative for IGF-IR (from patient 8 in Table 1).

Biochemical effects of blockade of IGF-IR signaling in mantle cell lymphoma

We performed western blotting of downstream targets of IGF-IR after treatment with PPP (results for the Mino cell line are shown as a representative example in Figure 5A). PPP induced down-regulation of pAkt and pIRS-1 without altering their total protein levels. In addition, PPP induced changes in apoptosis and cell cycle regulatory proteins. We noticed cleavage of the pro-apoptotic molecules caspase-3, caspase-8, caspase-9, and PARP. In addition, treatment with PPP was associated with increased cytosolic and decreased mitochondrial fractions of cytochrome c. Inhibition of IGF-IR by PPP also induced down-regulation of pCdc2 and up-regulation of cyclin B1, changes that are consistent with the occurrence of G2/M-phase cell cycle arrest.

Small molecule inhibitors, such as PPP, can induce non-specific effects. Therefore, experiments based on specific approaches were performed using siRNA. Cells were treated with either scrambled or IGF-IR siRNA. At 48 h, treatment with IGF-IR siRNA, and not scrambled siRNA, induced a significant decrease in IGF-IR (Figure 5B). The decrease in IGF-IR by siRNA was associated with decreases in pAkt, pJnk, and pIRS-1. Treatment of MCL cell lines with IGF-IR siRNA also increased cyclin B1 and decreased cyclin D1 levels. Finally, there was cleavage of both caspase-3 and PARP.

Discussion

We have attempted to provide evidence that IGF-IR plays an important role in maintaining the survival of MCL. We found that IGF-IR is over-expressed in MCL cell lines. These cell lines have been developed from MCL patients, and were previously described and characterized.[29] IGF-IR mRNA and protein were remarkably more expressed in MCL cell lines than in normal human B-lymphocytes. Furthermore, we explored whether IGF-IR was phosphorylated/activated in these cells, and the cell lines revealed receptor phosphorylation. We also studied the expression of IGF-IR and pIGF-IR in primary specimens from 23 MCL patients. The expression of IGF-IR and pIGF-IR was detected in 78% and 74%, respectively, of these specimens. Importantly, of the IGF-IR- and pIGF-IR-positive specimens, 72% were from MCL patients who presented with a clinical history of considerable resistance to previously administered therapeutic regimens, including some of the more aggressive regimens such as combined R-hyper-CVAD. Statistical analysis to explore whether significant differences exist between the survival of IGF-IR/pIGF-IR-positive patients and IGF-IR/pIGF-IR-negative ones was not conclusive, which was most likely because of the relatively small number of patients, particularly in the negative group.

A mechanism explaining the up-regulation of IGF-IR in MCL cells compared to in normal human B-lymphocytes has yet to be elucidated. It was previously shown that not only constitutive activation *per se*, but also the number of IGF-IR molecules per cell appears to play a very important role in the transformation properties of IGF-IR; this phenomenon is considered unusual among receptor tyrosine kinases. In line with this observation, *in vitro* and *in vivo* studies in mice showed that only a small increment in the number of IGF-IR molecules per cell can initiate transformation[36,37] In our study, MCL cell lines displayed a pronounced increase in the number of IGF-IR molecules/cell relative to the human B-lymphocytes. However, the levels of expres-

Table 1. Demographic data, specimen types, clinical presentations at time of biopsy, and status of expression of IGF-IR and pIGF-IR in MCL patients.

	Gender	Age	Specimen type	Presentation at time of specimen collection	IGF-IR	pIGF-IR
1	M	64	Hypopharyngeal mass, left	Relapsed after hyper-CVAD/rituximab	Positive	Positive
2	M	71	Spleen	Relapsed after hyper-CVAD/rituximab	Positive	Positive
3	F	66	Submandibular lymph node, left	Diagnostic biopsy, previously untreated	Negative	Negative
4	M	88	Multiple cervical lymph nodes	Resistant to rituximab, fludarabine, cyclophosphamide, and methotrexate	Positive	Positive
5	F	65	Posterior cervical lymph node, right	Diagnostic biopsy, previously untreated	Positive	Positive
6	F	67	Axillary lymph node, left	Resistant to hyper-CVAD/rituximab	Negative	Negative
7	M	51	Cervical lymph node, right	Relapsed after CHOP/rituximab (initially diagnosed with diffuse large B-cell lymphoma)	Positive	Positive
8	M	68	Supraclavicular lymph node, left; and peripheral blood	Diagnostic biopsy, previously untreated	Negative	Negative
9	M	71	Upper cervical lymph node, right	Relapsed after hyper-CVAD/rituximab	Positive	Positive
10	M	57	Parotid lymph node, right	Resistant to hyper-CVAD/rituximab	Positive	Positive
11	F	57	Submandibular lymph node	Diagnostic biopsy, previously untreated	Positive	Positive
12	F	46	Axillary lymph node, left	Resistant to CHOP/rituximab (initially diagnosed with chronic lymphocytic leukemia with MCL features)	Positive	Positive
13	M	62	Spleen	Resistant after several different combination chemotherapeutic regimens	Negative	Negative
14	M	55	Cervical lymph node, left	Diagnostic biopsy, previously untreated	Positive	Negative
15	M	58	Axillary lymph node, left	Relapsed after hyper-CVAD/rituximab	Negative	Negative
16	M	65	Inferior mediastinal lymph node	Relapsed after radiation therapy and fludarabine-based chemotherapeutic regimen	Positive	Positive
17	M	71	Axillary lymph node, left	Diagnostic biopsy, previously untreated	Positive	Positive
18	M	68	Mediastinal lymph node	Relapsed after hyper-CVAD, methotrexate, and ara-C	Positive	Positive
19	M	76	Iliac lymph nodes, right	Diagnostic biopsy, previously untreated	Positive	Positive
20	M	80	Soft tissue mass, right arm	Relapsed after rituximab, cyclophosphamide, mitoxantrone, vincristine, bortezomib, and doxorubicin	Positive	Positive
21	M	53	Bone marrow and peripheral blood	Relapsed after CHOP/rituximab	Positive	Positive
22	M	74	Bone marrow and peripheral blood	Relapsed after CHOP/rituximab	Positive	Positive
23	M	61	Peripheral blood	Relapsed after hyper-CVAD/rituximab	Positive	Positive

Excluding patient 23, expression of IGF-IR and pIGF-IR was determined by using immunohistochemical staining of tissue or bone marrow biopsies. For patient 23, the expression of IGF-IR and pIGF-IR was established based on western blot analysis of peripheral blood primary MCL cells after separation by cell sorting (Figure 1G).

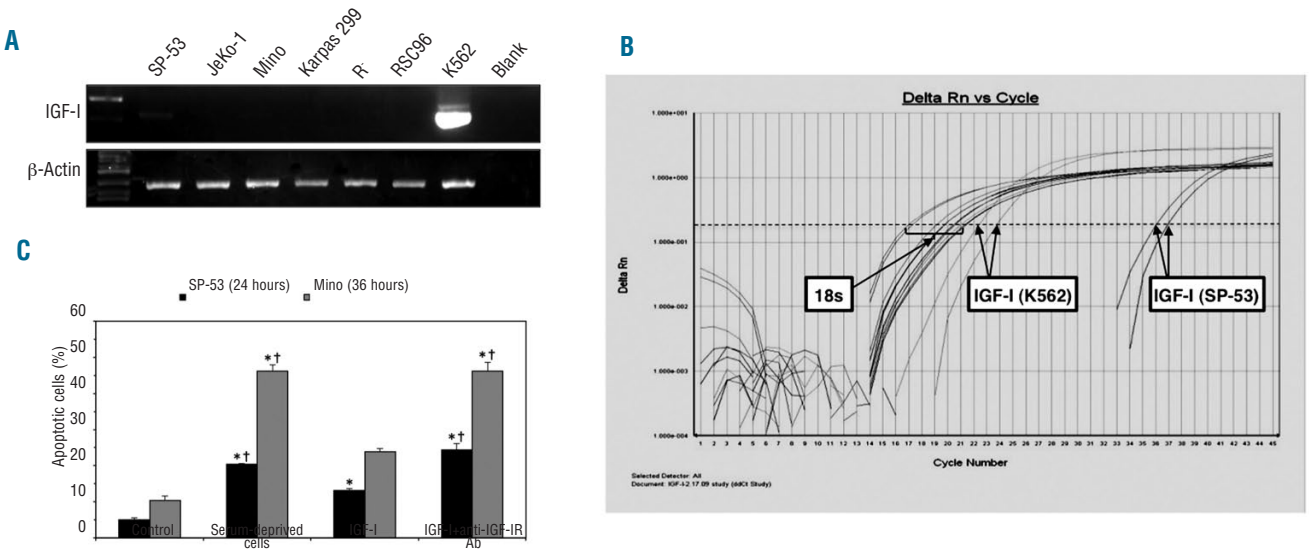

Figure 2. Lack of expression of IGF-I in MCL cell lines and effect of IGF-I on serum-deprived MCL cell lines. RT-PCR demonstrated lack of expression of IGF-I by JeKo-1 and Mino cell lines, and very low levels of expression by SP-53. R^- and RSC96 cell lines were used as negative controls and the K562 cell line as a positive control (A). In addition, qPCR was performed using 18s ribosomal RNA as an endogenous control. JeKo-1 and Mino cell lines demonstrated lack of expression, and SP-53 showed very low but negligible expression of IGF-I. RSC96 and K562 cell lines were used as negative and positive controls, respectively (B). Treatment of SP-53 and Mino cell lines with IGF-I after serum deprivation for 24 h salvaged these cells from apoptotic cell death. Simultaneous treatment of these cells with IGF-I and anti-IGF-IR blocking antibody diminished this effect. Results shown are means ± SD of two consistent experiments (*: $P<0.05$ *versus* control; †: $P<0.05$ *versus* IGF-I) (C).

sion of IGF-IR and pIGF-IR proteins and number of IGF-IR molecules per cell varied among the three cell lines, with levels of expression being lowest in the SP-53 cell line. These results suggest that the IGF-IR signaling axis may not be as activated in SP-53 as it is in JeKo-1 and Mino cell lines. Indeed, SP-53 cells were generally less responsive when treated with the IGF-IR inhibitor PPP. Similarly, Barnes *et al.* showed that head and neck cancer cell lines that expressed lower levels of IGF-IR were less responsive to IGF-IR inhibitors.[38]

IGF-I is the primary ligand for IGF-IR. Previous studies have proposed both IGF-I-dependent mechanisms through ligand-receptor interaction as well as IGF-I-independent mechanisms through a constitutively active receptor to initiate the IGF-IR-dependent signaling cascade.[39] We, therefore, wanted to determine whether autocrine secretion of IGF-I was involved in the activation of IGF-IR in MCL cells. There was no apparent expression of IGF-I by JeKo-1 and Mino cells and probable negligible expression by SP-53 cells. The expression of *IGF-IR* mRNA (*data not shown*) and IGF-IR and pIGF-IR proteins was also detected in serum-deprived MCL cell lines, suggesting that the expression and activation of IGF-IR are not necessarily dependent on the presence of IGF-I in the surrounding microenvironment. However, it has been shown that circulating IGF-I is increased in cancer patients,[40-41] and it is still possible that the release of IGF-I from surrounding lymph node stromal cells or from remote sources such as liver parenchyma could induce further enhancement of IGF-IR signaling in MCL. It is of note that circulating IGF-I levels are not known in patients with lymphoma, including those with MCL, and it will be of great interest to systematically explore these levels in future studies. Nonetheless, when serum-deprived MCL cell lines were treated with increasing concentrations of exogenous IGF-I, apoptosis decreased in comparison to untreated cells. These results provide evidence that the IGF-IR signaling axis is functional in MCL. In addition, the anti-apoptotic effects exerted by IGF-I were markedly diminished upon addition of an IGF-IR blocking antibody. This is especially important because it indicates that the effects seen upon treatment with IGF-I were not induced through parallel stimulation of the insulin receptor, which can be

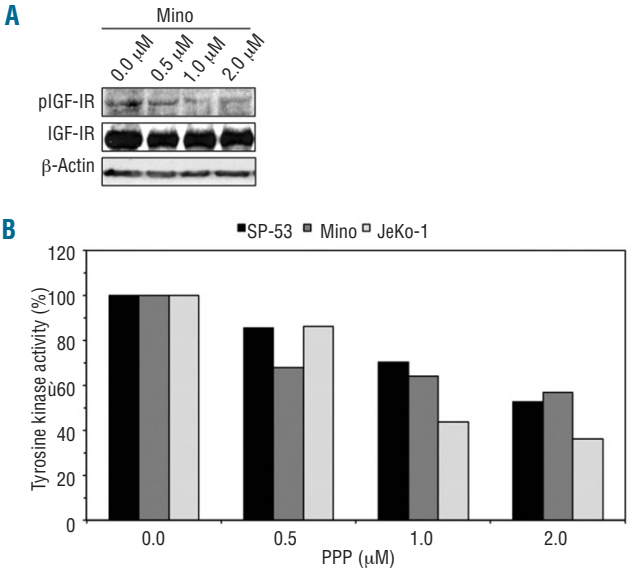

Figure 3. PPP decreases pIGF-IR and IGF-IR tyrosine kinase activity in MCL cell lines. Western blotting in the Mino cell line shows that PPP induces a concentration-dependent decrease in pIGF-IR at 24 h without affecting the basal levels of IGF-IR protein. The results are representative of three similar experiments (A). In addition, PPP reduced IGF-IR tyrosine kinase activity in a concentration-dependent manner at 24 h (B).

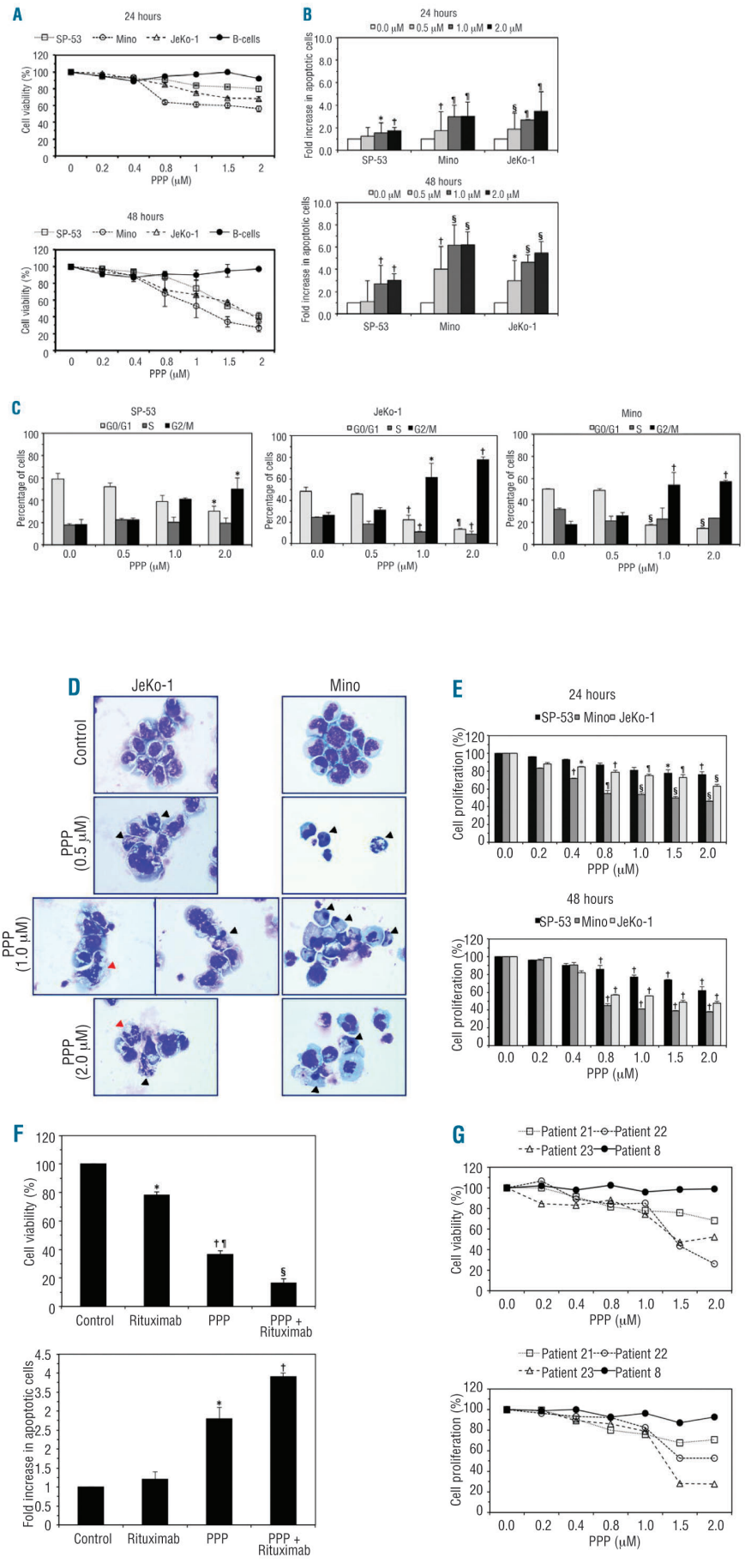

Figure 4. Cellular effects of inhibition of IGF-IR in MCL. PPP induced concentration-dependent decreases in the viability of MCL cell lines. At 24 h, excluding the 0.2 μM concentration of PPP in JeKo-1, and the 0.2 and 0.4 μM concentrations in Mino, all other concentrations induced statistically significant decreases in cell viability compared with untreated cells ($P<0.01$). At 48 h, PPP induced significant decreases in the viability of JeKo-1 and Mino cells ($P<0.001$ for all concentrations). In SP-53 cells, the decrease became statistically significant at 1.5 and 2.0 μM concentrations ($P<0.5$ and $P<0.01$, respectively), which was probably because of the greater variability of the response of this cell line to the lower concentrations of PPP (A). PPP also caused a concentration-dependent increase in apoptotic cells in MCL cell lines at 24 h, an effect which became more pronounced at 48 h (B). In addition, treatment with PPP was associated with G2/M-phase cell cycle arrest that became more significant with increasing concentrations of PPP (C). Figure 4. Compared with SP-53, the effects of PPP were generally more evident in Mino and JeKo-1 cell lines. The results are shown as means±SD (*$P<0.05$; †$P<0.01$; ¶: $P<0.001$; §$P<0.0001$ *versus* control cells). Morphological features consistent with apoptosis (black arrowheads) including cell shrinkage, nuclear condensation, and cytoplasmic vacuolization were seen after treatment with PPP (D). Also, atypical mitotic figures (red arrowheads) consistent with G2/M-phase cell cycle arrest were associated with treatment with PPP (D). PPP also decreased MCL cell proliferation in time- and concentration-dependent fashions (*:$P<0.05$; †: $P<0.01$; ¶: $P<0.001$; §: $P<0.0001$ *versus* control cells) (E). At 48 h, rituximab induced a significant decrease in the viability of JeKo-1 cells. However, the effect of PPP was more pronounced. Combined treatment with PPP and rituximab induced a marked decrease in the viability of these cells (*$P<0.01$ *versus* control and PPP + rituximab; †$P<0.001$ *versus* control and rituximab; ¶$P<0.01$ *versus* PPP + rituximab; §$P<0.001$ *versus* control) (F, upper panel). At 24 h, treatment of JeKo-1 cells with rituximab alone did not induce a significant increase in apoptotic cells. In contrast, PPP induced a significant increase in apoptotic cells compared with control and cells treated with rituximab alone. Furthermore, combined treatment with PPP and rituximab further enhanced apoptotic cell death (*$P<0.01$ *versus* control, rituximab, and PPP + rituximab; †$P<0.001$ *versus* control and rituximab) (F, lower panel). PPP induced a concentration-dependent decrease in the viability and proliferation of primary MCL cells that expressed IGF-IR. In contrast, PPP had minimal effects on MCL cells that were negative for IGF-IR (patients are shown in Table 1) (G).

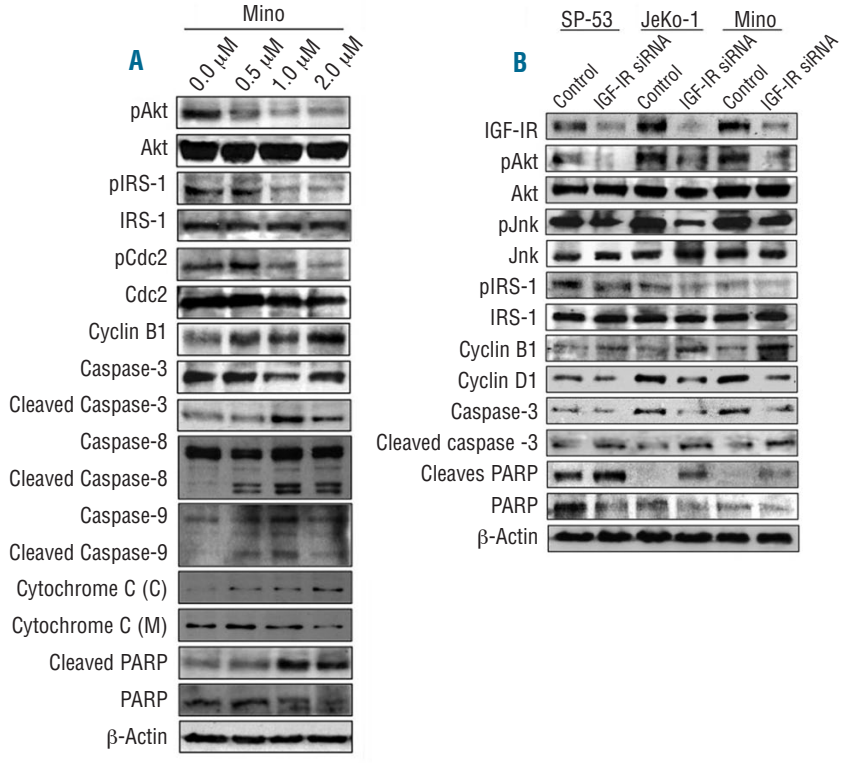

Figure 5. Effects of inhibition of IGF-IR on downstream targets in MCL cell lines. At 24 h, PPP induced a concentration-dependent down-regulation of pAkt and pIRS-1 without affecting their basal levels in the Mino cell line (A). PPP also decreased pCdc2 and increased cyclin B1, which is consistent with the occurrence of G2/M-phase cell cycle arrest. In support of apoptotic cell death, PPP caused cleavage of caspase-3, caspase-8, caspase-9, and PARP, which was associated with a decrease in their basal levels. Treatment with PPP was also associated with cytochrome c release resulting in increased cytosolic [C] fraction and decreased mitochondrial [M] fraction (A). Treating MCL cell lines with IGF-IR siRNA, and not control scrambled siRNA, for 48 h induced similar effects on some of these proteins and, in addition, decreased pJnk and cyclin D1 levels (B).

stimulated by very high levels of IGF-I.

That IGF-IR is important for the survival of MCL was demonstrated through experiments using PPP, a small molecule inhibitor of IGF-IR.[5] It was previously shown that PPP does not interfere with the highly homologous insulin receptor.[5] PPP does not selectively inhibit IGF-IR tyrosine kinase at the level of ATP binding; instead, it acts through inhibition of the activation loop of the IGF-IR kinase domain. Although the effects of PPP on other kinases are not entirely known, we recently demonstrated that PPP failed to decrease the phosphorylation or tyrosine kinase activity of BCR-ABL.[23] It is important to mention that PPP (AXL1717) is currently being used with promising success in phase I clinical trials that include patients with advanced non-small cell lung cancer.[18,42] After treatment of MCL cells lines using gradually increasing concentrations of PPP, we found reduced phosphorylation and kinase activity of IGF-IR. Down-regulation of IGF-IR signaling by PPP was associated with decreased cell viability and cell proliferation, apoptosis, and G2/M-phase cell cycle arrest. When we sought biochemical explanations for these effects, we found that PPP-mediated inhibition of IGF-IR was associated with cleavage of caspase-3, caspase-9 and PARP, release of cytochrome c, up-regulation of cyclin B1, and down-regulation of cyclin D1 and pCdc2. These effects are concordant with the occurrence of apoptosis and G2/M-phase cell cycle arrest. PPP also induced a significant decrease in the downstream oncogenic proteins pIRS-1 and pAkt. These effects were further confirmed using IGF-IR siRNA.

The changes observed in IGF-IR downstream target proteins after treating MCL cell lines with PPP are supportive of apoptotic cell death. Our results showed that the apoptosis induced by PPP was executed via activation of the extrinsic and intrinsic pathways. It was previously shown that IGF-IR signaling promotes anti-apoptotic effects by activation of survival signaling pathways, including IRS-1/PI3K/Akt, JAK/STAT, and Ras/MAPK, which induce significant inhibitory effects on both the extrinsic and intrinsic apoptotic pathways.[43] Of particular interest are the findings in the IRS-1 docking protein, which plays an essential role in IGF-IR downstream signaling through binding with the Y950 residue of the IGF-IRβ subunit. Upon phosphorylation, IRS-1 activates the p85 regulatory subunit of PI-3K, leading to activation of important downstream substrates including the p70 S6 kinase and Akt. To our knowledge, this is the first report documenting the expression of IRS-1 and pIRS-1 in MCL, which suggests that these proteins, through interactions with IGF-IR, could contribute to the survival of this aggressive lymphoma.

The occurrence of G2/M-phase cell cycle arrest after inhibition of IGF-IR by PPP is intriguing. We and others have previously reported similar effects of PPP on cell cycle progression in other types of hematologic malignancies.[20,22,23] It is possible that the changes observed in cell cycle regulatory proteins as well as the associated G2/M-phase cell cycle arrest are related to uncharacterized effects of PPP. However, this is unlikely to be the case because in the present study down-regulation of IGF-IR by siRNA also caused changes in cell cycle regulatory proteins reminiscent of those observed with PPP. IGF-IR has been shown to contribute to the progression of both the early and late phases of the cell cycle through interactions with cell cycle regulatory proteins.[44] For instance, Wu *et al.* demonstrated that the monoclonal anti-IGF-IR antibody A12 induces G1/S-phase cell cycle arrest in androgen-dependent prostatic tumors and G2/M-phase cell cycle arrest in androgen-independent ones, testifying to the fact that IGF-IR inhibition can result in cell cycle arrest at any phase of the cell cycle.[13] Considering that cyclin D1 is an early phase cell cycle regulatory protein and it is over-expressed in MCL primarily

because of the chromosomal translocation t(11;14)(q13;q32), it is surprising to see that down-regulation of IGF-IR caused G2/M-phase cell cycle arrest despite the decrease in cyclin D1 levels. The contribution of cyclin D1 to the initiation and progression of MCL is controversial. Some investigators have documented that cyclin D1 transgenic mice do not develop lymphoma without possessing additional molecular events such as coexistent *myc*, whereas others found that nuclear accumulation of cyclin D1 through experimentally induced mutations that interfere with its binding with CRM1 protein and subsequent nuclear export is a prerequisite for lymphoma development and this mechanism does not require any additional molecular events.[45-47] How cyclin D1 contributes to lymphomagenesis is, however, poorly understood. Regardless, one possible explanation for our observations is that the balance existing between early phase and late phase cell cycle regulatory proteins has been disrupted in favor of G2/M-phase cell cycle arrest after inhibition of IGF-IR in MCL cells. This important finding needs further investigations.

Our data suggest that targeting IGF-IR may represent a reasonable strategy to treat MCL patients. To further explore this possibility, we employed two different experimental approaches. In the first, we sought to explore whether targeting IGF-IR would enhance the effects of rituximab, one of the drugs currently used to treat MCL patients. We elected to use the JeKo-1 cell line in these experiments because this cell line demonstrated a response to PPP that was intermediate between those of the SP-53 and Mino cell lines. Although treatment with rituximab or PPP induced a significant decrease in the viability of JeKo-1 cells, combined treatment further enhanced this effect. Previous *in vitro* studies demonstrated variable effects of rituximab on apoptosis induction in B-cell lymphoma.[30-32] Experimental conditions including the presence of complement, duration of treatment, type of lymphoma, and treating primary lymphoma cells *versus* cell lines, appear to have influenced the outcome of these studies. In our experiments, rituximab alone did not induce a significant increase in apoptosis in JeKo-1 cells at 24 h after treatment. Nonetheless, treatment with PPP led to a marked increase in apoptosis, and this increase became more significant when cells were simultaneously treated with PPP and rituximab. In the second experimental approach, we tested the *in vitro* effects of PPP on primary MCL cells. PPP induced a concentration-dependent decrease in the viability and proliferation of these cells. However, the effect of PPP on cell viability was lacking in primary MCL cells that were negative for the expression of IGF-IR, which is in further support of the reasonable selectivity of PPP.

In conclusion, we provide evidence that IGF-IR is expressed and activated in MCL cell lines as well as in the majority of MCL primary samples including samples collected from patients who demonstrated considerable resistance to the currently utilized therapeutics. Importantly, IGF-IR signaling appears to contribute to the survival of MCL, and inhibition of IGF-IR induces MCL cell death. Taken together, our results suggest that targeting IGF-IR could represent a potential therapeutic strategy to be utilized for the treatment of MCL patients in the future.

Authorship and Disclosures

The information provided by the authors about contributions from persons listed as authors and in acknowledgments is available with the full text of this paper at www.haematologica.org.

Financial and other disclosures provided by the authors using the ICMJE (www.icmje.org) Uniform Format for Disclosure of Competing Interests are also available at www.haematologica.org.

References

1. Ullrich A, Gray A, Tam AW, Yang-Feng T, Tsubokawa M, Collins C, et al. Insulin-like growth factor I receptor primary structure: comparison with insulin receptor suggests structural determinants that define functional specificity. EMBO J. 1986;5(10):2503-12.
2. De Meyts P, Whittaker J. Structural biology of insulin and IGF1 receptors: implications for drug design. Nat Rev Drug Discov. 2002;1(10):769-83.
3. Kato H, Faria TN, Stannard B, Roberts CT Jr, LeRoith D. Essential role of tyrosine residues 1131, 1135, and 1136 of the insulin-like growth factor-I (IGF-I) receptor in IGF-I action. Mol Endocrinol. 1994;8(1): 40-50.
4. Peruzzi F, Prisco M, Dews M, Salomoni P, Grassilli E, Romano G, et al. Multiple signaling pathways of the insulin-like growth factor 1 receptor in protection from apoptosis. Mol Cell Biol. 1999;19(10):7203-15.
5. Vasilcanu D, Girnita A, Girnita L, Vasilcanu R, Axelson M, Larsson O. The cyclolignan PPP induces activation loop-specific inhibition of tyrosine phosphorylation of the insulin-like growth factor-1 receptor. Link to phosphatidyl inositol-3 kinase/Akt apoptotic pathway. Oncogene. 2004;23(47): 7854-62.
6. Zong CS, Chan J, Levy DE, Horvath C, Sadowski HB, Wang LH. Mechanism of STAT3 activation by insulin-like growth factor I receptor. J Biol Chem. 2000;275(20): 15099-105.
7. Gual P, Baron V, Lequoy V, Van Obberghen E. Interaction of Janus kinases JAK-1 and JAK-2 with the insulin receptor and the insulin-like growth factor-1 receptor. Endocrinology. 1998;139(3):884-93.
8. Samani AA, Yakar S, LeRoith D, Brodt P. The role of the IGF system in cancer growth and metastasis: overview and recent insights. Endocr Rev. 2007;28(1):20-47.
9. Baserga R, Sell C, Porcu P, Rubini M. The role of the IGF-I receptor in the growth and transformation of mammalian cells. Cell Prolif. 1994;27(2):63-71.
10. Sell C, Rubini M, Rubin R, Liu JP, Efstratiadis A, Baserga R. Simian virus 40 large tumor antigen is unable to transform mouse embryonic fibroblasts lacking type 1 insulin-like growth factor receptor. Proc Natl Acad Sci USA. 1993;90(23):11217-21.
11. Toretsky JA, Kalebic T, Blakesley V, LeRoith D, Helman LJ. The insulin-like growth factor-I receptor is required for EWS/FLI-1 transformation of fibroblasts. J Biol Chem. 1997;272(49):30822-7.
12. Lu Y, Zi X, Zhao Y, Mascarenhas D, Pollak M. Insulin-like growth factor-I receptor signaling and resistance to trastuzumab (Herceptin). J Natl Cancer Inst. 2001;93(24): 1852-7.
13. Wu JD, Odman A, Higgins LM, Haugk K, Vessella R, Ludwig DL, et al. In vivo effects of the human type I insulin-like growth factor receptor antibody A12 on androgen-dependent and androgen-independent xenograft human prostate tumors. Clin Cancer Res. 2005;11(8):3065-74.
14. Iwasa T, Okamoto I, Suzuki M, Hatashita E, Yamada Y, Fukuoka M, et al. Inhibition of insulin-like growth factor 1 receptor by CP-751,871 radiosensitizes non-small cell lung cancer cells. Clin Cancer Res. 2009;15 (16):5117-25.
15. Coppola D, Saunders B, Fu L, Mao W, Nicosia SV. The insulin-like growth factor 1 receptor induces transformation and tumorigenicity of ovarian mesothelial cells and down-regulates their Fas-receptor expression. Cancer Res. 1999;59(13):3264-70.
16 Wilker E, Bol D, Kiguchi K, Rupp T, Beltrán L, DiGiovanni J. Enhancement of susceptibility to diverse skin tumor promoters by activation of the insulin-like growth factor-1 receptor in the epidermis of transgenic mice. Mol Carcinog. 1999;25(2):122-31.
17. Gualberto A, Pollak M. Clinical development of inhibitors of the insulin-like growth factor receptor in oncology. Curr Drug Targets. 2009;10(10):923-36.
18. Gualberto A, Pollak M. Emerging role of

insulin-like growth factor receptor inhibitors in oncology: early clinical trial results and future directions. Oncogene. 2009;28(34): 3009-21.
19. Bertrand FE, Steelman LS, Chappell WH, Abrams SL, Shelton JG, White ER, et al. Synergy between an IGF-1R antibody and Raf/MEK/ERK and PI3K/Akt/mTOR pathway inhibitors in suppressing IGF-1R-mediated growth in hematopoietic cells. Leukemia. 2006;20(7):1254-60.
20. Strömberg T, Ekman S, Girnita L, Dimberg LY, Larsson O, Axelson M, et al. IGF-1 receptor tyrosine kinase inhibition by the cyclolignan PPP induces G2/M-phase accumulation and apoptosis in multiple myeloma cells. Blood. 2006;107(2):669-78.
21. Menu E, Jernberg-Wiklund H, Strömberg T, De Raeve H, Girnita L, Larsson O, et al. Inhibiting the IGF-1 receptor tyrosine kinase with the cyclolignan PPP: an in vitro and in vivo study in the 5T33MM mouse model. Blood. 2006;107(2):655-60.
22. Shi P, Lai R, Lin Q, Iqbal AS, Young LC, Kwak LW, et al. IGF-IR tyrosine kinase interacts with NPM-ALK oncogene to induce survival of T-cell ALK+ anaplastic large-cell lymphoma cells. Blood. 2009;114 (2):360-70.
23. Shi P, Chandra J, Sun X, Gergely M, Cortes JE, Garcia-Manero G, et al. Inhibition of IGF-IR tyrosine kinase induces apoptosis and cell cycle arrest in imatinib-resistant chronic myeloid leukemia cells. J Cell Mol Med. 2010;14(6B):1777-92.
24. Tazzari PL, Tabellini G, Bortul R, Papa V, Evangelisti C, Grafone T, et al. The insulin-like growth factor-I receptor kinase inhibitor NVP-AEW541 induces apoptosis in acute myeloid leukemia cells exhibiting autocrine insulin-like growth factor-I secretion. Leukemia. 2007;21(5):886-96.
25. Wahner Hendrickson AE, Haluska P, Schneider PA, Loegering DA, Peterson KL, Attar R, et al. Expression of insulin receptor isoform A and insulin-like growth factor-1 receptor in human acute myelogenous leukemia: effect of the dual-receptor inhibitor BMS-536924 in vitro. Cancer Res. 2009;69(19):7635-43.
26. Fernàndez V, Hartmann E, Ott G, Campo E, Rosenwald A. Pathogenesis of mantle-cell lymphoma: all oncogenic roads lead to dysregulation of cell cycle and DNA damage response pathways. J Clin Oncol. 2005;23 (26):6364-9.
27. Jares P, Colomer D, Campo E. Genetic and molecular pathogenesis of mantle cell lymphoma: perspectives for new targeted therapeutics. Nat Rev Cancer. 2007;7(10):750-62.
28. Williams ME, Dreyling MH, Kahl BS, Leonard JP, O'Connor OA, Press OW, et al. Mantle cell lymphoma: report of the 2009 Mantle Cell Lymphoma Consortium Workshop. Leuk Lymphoma. 2010;51(3): 390-8.
29. Amin HM, McDonnell TJ, Medeiros LJ, Rassidakis GZ, Leventaki V, O'Connor SL, et al. Characterization of 4 mantle cell lymphoma cell lines: establishment of an in vitro study model. Arch Pathol Lab Med. 2003;127(4):424-31.
30. Bellosillo B, Villamor N, López-Guillermo A, Marcé S, Esteve J, Campo E, et al. Complement-mediated cell death induced by rituximab in B-cell lymphoproliferative disorders is mediated in vitro by a caspase-independent mechanism involving the generation of reactive oxygen species. Blood. 2001;98(9):2771-7.
31. Rose AL, Smith BE, Maloney DG. Glucocorticoids and rituximab in vitro: synergistic direct antiproliferative and apoptotic effects. Blood. 2002;100(5):1765-73.
32. Manches O, Lui G, Chaperot L, Gressin R, Molens JP, Jacob MC, et al. In vitro mechanisms of action of rituximab on primary non-Hodgkin lymphomas. Blood. 2003;101 (3):949-54.
33. Qiu L, Lai R, Lin Q, Lau E, Thomazy DM, Calame D, et al. Autocrine release of interleukin-9 promotes Jak3-dependent survival of ALK+ anaplastic large-cell lymphoma cells. Blood. 2006;108(7):2407-15.
34. Amin HM, Hoshino K, Yang H, Lin Q, Lai R, Garcia-Manero G. Decreased expression level of SH2 domain-containing protein tyrosine phosphatase-1 (Shp1) is associated with progression of chronic myeloid leukaemia. J Pathol. 2007;212(4):402-10.
35. Rosengren L, Vasilcanu D, Vasilcanu R, Fickenscher S, Sehat B, Natalishvili N, et al. IGF-1R tyrosine kinase expression and dependency in clones of IGF-1R knockout cells (R-). Biochem Biophys Res Commun. 2006;347(4):1059-66.
36. Rubini M, Hongo A, D'Ambrosio C, Baserga R. The IGF-I receptor in mitogenesis and transformation of mouse embryo cells: role of receptor number. Exp Cell Res. 1997; 230(2):284-92.
37. Flossmann-Kast BB, Jehle PM, Hoeflich A, Adler G, Lutz MP. Src stimulates insulin-like growth factor I (IGF-I)-dependent cell proliferation by increasing IGF-I receptor number in human pancreatic carcinoma cells. Cancer Res. 1998;58(16):3551-4.
38. Barnes CJ, Ohshiro K, Rayala SK, El-Naggar AK, Kumar R. Insulin-like growth factor receptor as a therapeutic target in head and neck cancer. Clin Cancer Res. 2007;13(14): 4291-99.
39. Nair PN, De Armond DT, Adamo ML, Strodel WE, Freeman JW. Aberrant expression and activation of insulin-like growth factor-1 receptor (IGF-1R) are mediated by an induction of IGF-1R promoter activity and stabilization of IGF-1R mRNA and contributes to growth factor independence and increased survival of the pancreatic cancer cell line MIA PaCa-2. Oncogene. 2001;20 (57):8203-14.
40. Bergmann U, Funatomi H, Yokoyama M, Beger HG, Korc M. Insulin-like growth factor I overexpression in human pancreatic cancer: evidence for autocrine and paracrine roles. Cancer Res. 1995;55(10): 2007-11.
41. Manousos O, Souglakos J, Bosetti C, Tzonou A, Chatzidakis V, Trichopoulos D, et al. IGF-I and IGF-II in relation to colorectal cancer. Int J Cancer. 1999;83(1):15-7.
42. Ekman S, Frödin JE, Harmenberg J, Bergman A, Hedlund A, Dahg P, et al. Clinical phase I study with an insulin-like growth factor-1 receptor inhibitor: experiences in patients with squamous non-small lung carcinoma. Acta Oncol. 2011;50(3): 441-7.
43. Kooijman R. Regulation of apoptosis by insulin-like growth factor (IGF)-I. Cytokine Growth Factor Rev. 2006;17(4):305-23.
44. Hamelers IH, van Schaik RF, Sipkema J, Sussenbach JS, Steenbergh PH. Insulin-like growth factor I triggers nuclear accumulation of cyclin D1 in MCF-7S breast cancer cells. J Biol Chem. 2002;277(49):47645-52.
45. Bodrug SE, Warner BJ, Bath ML, Lindeman GJ, Harris AW, Adams JM. Cyclin D1 impedes lymphocyte maturation and collaborates in lymphomagenesis with the myc gene. EMBO J. 1994;13(9):2124-30.
46. Lovec H, Grzeschiczek A, Kowalski M-B, Moroy T. Cyclin D1/bcl-1 cooperates with myc genes in the generation of B-cell lymphoma in transgenic mice. EMBO J. 1994;13(15):3487-95.
47. Gladden AB, Woolery R, Aggarwal P, Wasik MA, Diehl JA. Expression of constitutively nuclear cyclin D1 in murine lymphocytes induces B-cell lymphoma. Oncogene. 2006;25(7):998-1007.